Suplemento de la Revista Mexicana de Física **3** 0308040 (2022) 1–5

The effect of hidden-charm strange pentaquarks p_{cs} on the $k^- p \to j/\psi\, \lambda$ reaction

Samson Clymton, Hee-Jin Kim and Hyun-Chul Kim
Hadron Theory Group, Department of Physics, Inha University, Incheon 22212, Republic of Korea.

Received 10 January 2022; accepted 1 March 2022

We present a recent investigation on the production of $P_{cs}(4459)$ in the $K^- p \to J/\psi\Lambda$ reaction, using both the effective Lagrangian and Regge approaches. We assume six different spin and parity assignments, *i.e.*, $1/2^{\pm}$, $3/2^{\pm}$ and $5/2^{\pm}$ to the newly found P_{cs}. The total and differential cross sections for the $K^- p \to J/\psi\Lambda$ reaction are calculated. We examine the dependence of the results on the different assignments of J^P for P_{cs}.

Keywords: Pentaquarks; $K^- p$ reaction; Regge approach.

DOI: https://doi.org/10.31349/SuplRevMexFis.3.0308040

1. Introduction

The strong decays of heavy mesons and baryons have offered a great deal of findings of exotic hadrons over the last decade. The first heavy pentaquark P_c is one of them, which was observed in the $\Lambda_b^0 \to J/\psi K^- p$ decay [1]. Very recently, the LHCb Collaboration sharpened the spectrum of the heavy pentaquarks by increasing the yields of Λ_b^0 [2] and found yet another heavy pentaquark that has strangeness in the analysis of the $\Xi_b^- \to J/\psi\Lambda K^-$ decay [3]. The mass and width of the hidden-charmed pentaquark with strangeness labeld as $P_{cs}^0(4459)$ were determined to be, respectively, $4458.8 \pm 2.9^{+4.7}_{-1.1}$ MeV and $17.3^{+8.0}_{-5.7}$ MeV. Its spin and parity are still unknown.

Before the new finding of $P_{cs}(4459)$ was announced, its existence had been predicted by many authors [4–10] (see also a recent review [11]). Since the mass of $P_{cs}^0(4459)$ is located below the $\bar{D}^*\Xi_c^0$ threshold energy by about 19 MeV, $P_{cs}^0(4459)$ may be interpreted as a molecular state of the Λ and J/ψ. This picture being assumed, the quantum number of P_{cs}^0 is proposed to be $1/2^-$ or $3/2^-$.

If the hidden-charm pentaquark P_c and P_{cs} exist, then one can also find them in the two-body processes. Actually, The GlueX Collaboration measure the J/ψ photoproduction off the nucleon, searching for the existence of the hidden-charmed pentaquarks P_c [12]. However, the results show no direct evidence of this exotic state. Furthermore, there is still no experimental program to investigate the production of the hidden-charmed pentaquarks through hadronic processes by using meson beams. On the other hand, there are several theoretical studies on the production of P_c in the $\pi^- p \to J/\psi n$ reaction. They provide a simple mechanism as to how P_c's are produced [13, 14]. One can carry out a similar investigation on the production of P_{cs}, using the kaon beam. This is the subject we discuss now.

In the present talk, we report a recent investigation on the production of the hidden-charmed pentaquarks with strangeness P_{cs} in the $K^- p \to J/\psi\Lambda$ reaction. Employing two different methods, *i.e.*, the effective Lagrangian and Regge approaches, we are able to compute the scattering amplitude of the $K^- p \to J/\psi\Lambda$ reaction. Then, we can directly predict the differential and total cross sections. Since the energy of the threshold is already high enough, the hybridized Regge approach is a very plausible method to study the $J/\psi\Lambda$ production [15–17]. Because the spin-parity quantum number of $P_{cs}^0(4459)$ is experimentally unknown, we will consider the spin-parity states up from $1/2^{\pm}$ to $5/2^{\pm}$. We scrutinize the different behaviors of the differential and total cross sections with the spin-parity states. The present study will provide a useful guidance for future experiments.

2. Formalism

2.1. Effective Lagrangian approach

The transition amplitude for $K^- p \to J/\psi\Lambda$ is derived from effective Lagrangian approach. We take the Born approximation, so that we calculate the tree-level exchange diagrams shown in Fig. 1. Since we are interested in the production of the heavy pentaquark $P_{cs}(4459)$, we include the P_{cs} pole diagram in the s-channel.

Moreover, since the spin-parity quantum numbers of $P_{cs}(4459)$ are unknown, we employ six different cases: $J^P = 1/2^{\pm}, 3/2^{\pm}, 5/2^{\pm}$. By considering these spin-parity assignments, the effective Lagrangian for the $P_{cs}\Lambda J/\psi$ vertex can be expressed as

$$\begin{aligned}
\mathcal{L}^{1/2\pm}_{P\Lambda J/\psi} &= -\, g_{P\Lambda J/\psi}\bar{P}\Gamma^{\mp}_{\mu}\Lambda\psi^{\mu} + \text{h.c.},\\
\mathcal{L}^{3/2\pm}_{P\Lambda J/\psi} &= -\,\frac{g_{P\Lambda J/\psi}}{2m_{\Lambda}}\bar{P}_{\mu}\Gamma^{\pm}_{\nu}\Lambda\left(\partial^{\mu}\psi^{\nu} - \partial^{\nu}\psi^{\mu}\right) + \text{h.c.},\\
\mathcal{L}^{5/2\pm}_{P\Lambda J/\psi} &= -\frac{g_{P\Lambda J/\psi}}{2m_{\Lambda}^2}\bar{P}_{\mu\alpha}\Gamma^{\mp}_{\nu}\Lambda\partial^{\alpha}\left(\partial^{\mu}\psi^{\nu} - \partial^{\nu}\psi^{\mu}\right) + \text{h.c.},
\end{aligned} \tag{1}$$

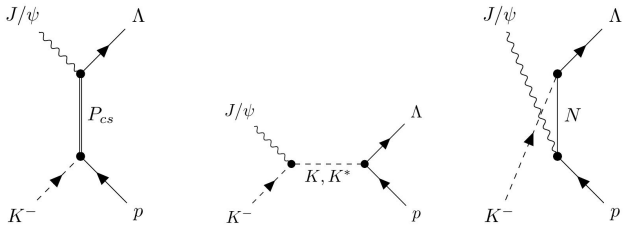

FIGURE 1. Tree-level Feynman diagrams used in the present work. The left, center and right parts correspond respectively to s-, t-, and u-channels.

where the P, Λ, and ψ^μ denote the $P_{cs}^0(4459)$, Λ^0, and J/ψ fields respectively. The Λ hyperon mass is labeled by m_Λ. The parity factors are given by

$$\Gamma^\pm = \begin{pmatrix} 1 \\ i\gamma_5 \end{pmatrix}, \qquad \Gamma^\pm_\mu = \begin{pmatrix} \gamma_\mu\gamma_5 \\ \gamma_\mu \end{pmatrix}. \tag{2}$$

The Lagrangian in Eq. (1) is already in the truncated form of that given in Ref. [18], where we neglect higher momentum terms. The $P_{cs}NK$ vertex is described by following effective Lagrangian:

$$\begin{aligned}
\mathcal{L}^{1/2\pm}_{PNK} &= -g_{PNK}\bar{P}\Gamma^\mp NK + \text{h.c.}, \\
\mathcal{L}^{3/2\pm}_{PNK} &= -\frac{g_{PNK}}{M\, m_N}\varepsilon^{\mu\nu\alpha\beta}\partial_\mu\bar{P}_\nu\Gamma^\pm_\alpha N\partial_\beta K + \text{h.c.}, \\
\mathcal{L}^{5/2\pm}_{PNK} &= -\frac{g_{PNK}}{M\, m_N^2}\varepsilon^{\mu\nu\alpha\beta}\partial_\mu\bar{P}_{\nu\rho}\Gamma^\mp_\alpha N\partial^\rho\partial_\beta K + \text{h.c.},
\end{aligned} \tag{3}$$

where M and m_N denote the masses corresponding respectively to P_{cs} and nucleon.

To determine the coupling constants in the Eq. (1) and (3), we need information on the branching fraction of P_{cs} decays. Unfortunately, there is no experimental data on the decay of P_{cs}. However, on the theoretical side, several studies have already predicted the branching ratio of P_{cs} decays to $J/\psi\Lambda$ [19, 20]. This help us to assume the branching ratio of the $P_{cs} \to J/\psi\Lambda$ is about 1 %. Furthermore, since the decay of P_{cs} to K^-p is OZI-suppressed process, we assume its branching ratio to be of order 0.01%. Having determined all the branching ratios, we are able to calculate the coupling constants for the $P_{cs}\Lambda J/\psi$ and $P_{cs}NK$ vertices, using the partial decay width formula [18]. The results are listed in Table I.

TABLE I. The coupling constants for $P_{cs}\Lambda J/\psi$ and $P_{cs}NK$ vertices by considering six different cases of spin-parity assignments of $P_{cs}^0(4459)$.

J^P	$g_{P\Lambda J/\psi}$	g_{PNK}
$1/2^-$	4.41×10^{-2}	3.77×10^{-3}
$1/2^+$	1.26×10^{-1}	5.82×10^{-3}
$3/2^-$	5.46×10^{-2}	3.18×10^{-3}
$3/2^+$	1.48×10^{-1}	2.06×10^{-3}
$5/2^-$	3.83×10^{-1}	1.19×10^{-3}
$5/2^+$	1.33×10^{-1}	1.84×10^{-3}

The non-resonance contribution to the transition amplitude for $K^-p \to J/\psi\Lambda$ come from K and K^* meson exchange in t-channel and nucleon exchange in u-channel depicted as in Fig. 1. The effective Lagrangian for each vertex in those diagrams is given by

$$\begin{aligned}
\mathcal{L}_{J/\psi KK} &= -ig_{J/\psi KK}\,\psi^\mu\left(K^+\partial_\mu K^- - K^-\partial_\mu K^+\right), \\
\mathcal{L}_{J/\psi KK^*} &= -\frac{g_{J/\psi KK^*}}{m_\psi}\varepsilon^{\mu\nu\alpha\beta}\partial_\mu\psi_\nu K\partial_\alpha K^*_\beta, \\
\mathcal{L}_{J/\psi NN} &= -g_{J/\psi NN}\bar{N}\gamma_\mu\psi^\mu N + \text{h.c.}, \\
\mathcal{L}_{\Lambda NK} &= -\frac{f_{\Lambda NK}}{m_\pi}\bar{\Lambda}\gamma_\mu\gamma_5 N\partial^\mu K + \text{h.c.}, \\
\mathcal{L}_{\Lambda NK^*} &= -g_{\Lambda NK^*}\bar{\Lambda}\gamma^\mu N K^*_\mu - \frac{f_{\Lambda NK^*}}{4m_N}\bar{\Lambda}\sigma^{\mu\nu}N \\
&\quad\times\left(\partial_\mu K^*_\nu - \partial_\nu K^*_\mu\right) + \text{h.c.}.
\end{aligned} \tag{4}$$

The coupling constants for $J/\psi KK$ and $J/\psi KK^*$ vertices are determined by the experimental data on theirs branching ratios [21] while the coupling constants for ΛNK and ΛNK^* vertices are taken directly from the Nijmegen model (ESC08a) [22]. Lastly, the coupling constant $g_{J/\psi NN}$ is obtained from Ref. [23].

Since the hadrons have finite sizes and the scattering amplitudes should satisfy the unitarity, we introduce a form factor at each vertice. We use the widely used form factor in reaction calculations as follows:

$$\begin{aligned}
F_s(s) &= \frac{\Lambda^4}{\Lambda^4 + (s-m^2)^2}, \\
F_t(t) &= \frac{\Lambda^2 - m^2}{\Lambda^2 - t}, \\
F_u(u) &= \frac{\Lambda^2 - m^2}{\Lambda^2 - u}.
\end{aligned} \tag{5}$$

The cutoff mass Λ is chosen by adding about 600 MeV to the exchange particle's mass [18]. So, we use a rather high cutoff mass $\Lambda_{P_{cs}} = 5.0$ GeV for P_{cs}-exchange.

2.2. Regge approach

In the present work we calculate the P_{cs} production by using the hybridized Regge approach. The hybridized Regge amplitude was suggested for the quantative description of the high-energy behaviours of the hadronic reactions [15]. This approach can be achieved by replacing the standard Feynman propagator with one from the Regge theory

$$\frac{1}{t - m_X^2} \to \mathcal{P}_{\text{Regge}} \equiv -\Gamma(-\alpha_X(t))\xi_X(t)\alpha'_X\left(\frac{s}{s_0}\right)^{\alpha_X(t)}, \tag{6}$$

where $\alpha_X(t)$ stands for the Regge trajectory of particle X. s_0 denotes the scale parameter.

The J/ψ production in K^-p scattering is strongly suppressed by OZI rule. Considering the quark components of

incident beams, we find that K and K^* Reggeon exchanges are relevant to be t-channel processes. One can determine the value of the s_0 employing the result of Model I as a guideline. Comparison of the $d\sigma/dt$ at the pole position between Model I and II results in $s_0 = 5$ GeV^2 and 2 GeV^2 for K and K^* exchange, respectively. In addition, we consider the nucleon Reggeon as a u-channel contribution. Since the asymtotic behavior of the Γ function does not allow large s_0, we fix the $s_0 = 2$ GeV^2.

In order to take the K and K^* Regge poles precisely, we utilize the nonlinear Regge trajectories as follows [24]:

$$\alpha_K(t) = \alpha_K(0) + \gamma\left(\sqrt{T_K} - \sqrt{T_K - t}\right), \qquad (7)$$

where γ is the universal slope and T_K indicates the point at which the Regge trajectory is terminated. The values of parameters are listed below.

$$\begin{aligned} \alpha_K(0) &= -0.151, \quad \alpha_{K^*}(0) = 0.414, \\ \sqrt{T_K} &= 2.96\ \text{GeV}, \quad \sqrt{T_{K^*}} = 2.58\ \text{GeV}, \\ \gamma &= 3.65\ \text{GeV}^{-1}. \end{aligned} \qquad (8)$$

As for the u-channel, we use the linear Regge trajectory. The values for the intercept and slope are given as

$$\alpha_N(0) = -0.384, \quad \alpha'_N = 0.996. \qquad (9)$$

3. Results and discussions

The total cross sections for the $K^- p \to J/\psi\Lambda$ reaction are calculated by using two different theoretical frameworks, effective Lagrangian (Model I) and hybridized Regge approach (Model II). In each model, we examine the dependence of the results on different assignments of J^P for P_{cs}. As shown in Figs. 2 and 3, the variation of J^P gives no change in the energy distribution shape of the total cross section for both models. Indeed, a significant difference of cross section occurs around the resonance mass. The reason can be found from the resonance and non-resonance interference part that

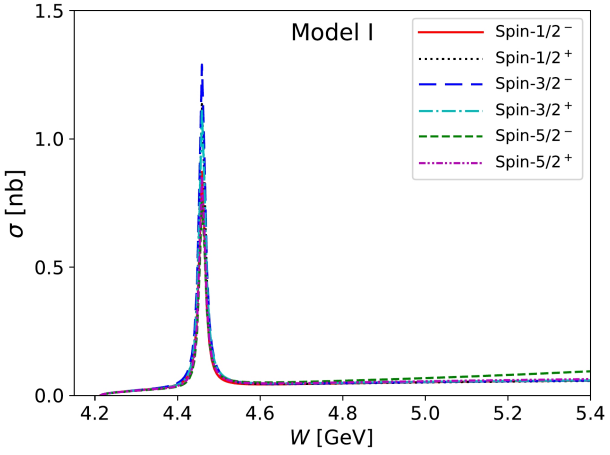

FIGURE 2. The calculated total cross section from Model I by taking into account six different assignments of spin-parity quantum number of $P^0_{cs}(4459)$.

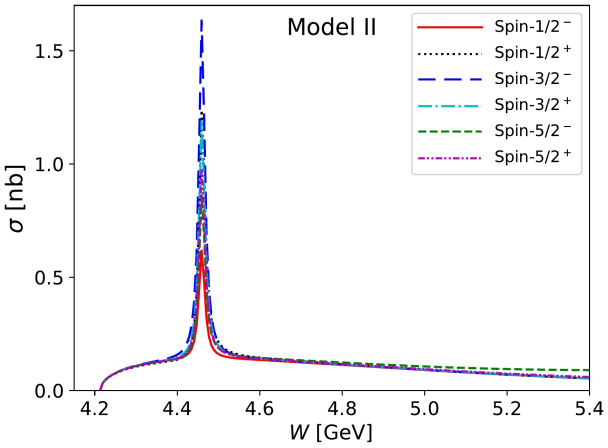

FIGURE 3. The calculated total cross section from Model II by taking into account six different assignments of spin-parity quantum number of $P^0_{cs}(4459)$.

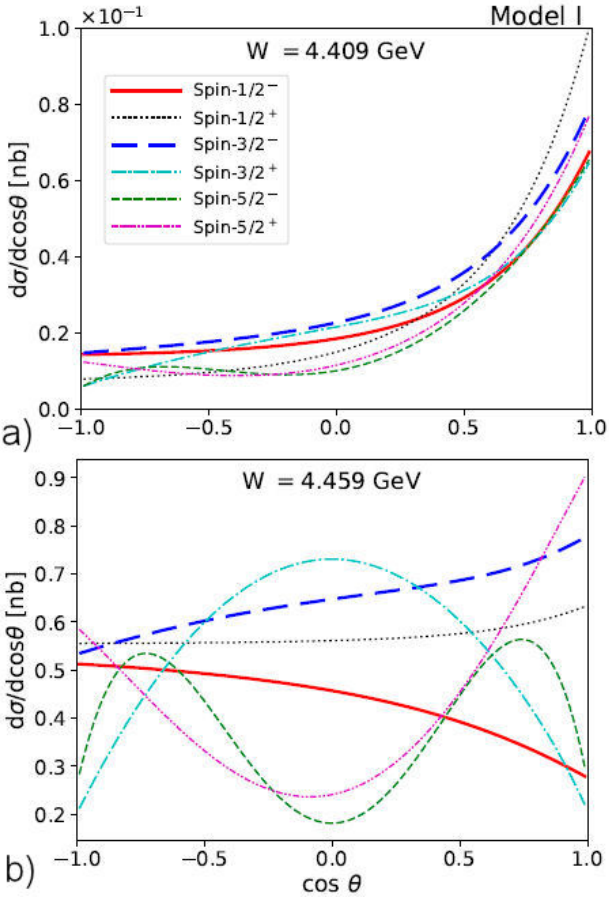

FIGURE 4. The calculated differential cross section ($d\sigma/d\Omega$) as a function of scattering angle θ for a given total energy W from Model I by taking into account six different assignments of spin-parity quantum number of $P^0_{cs}(4459)$.

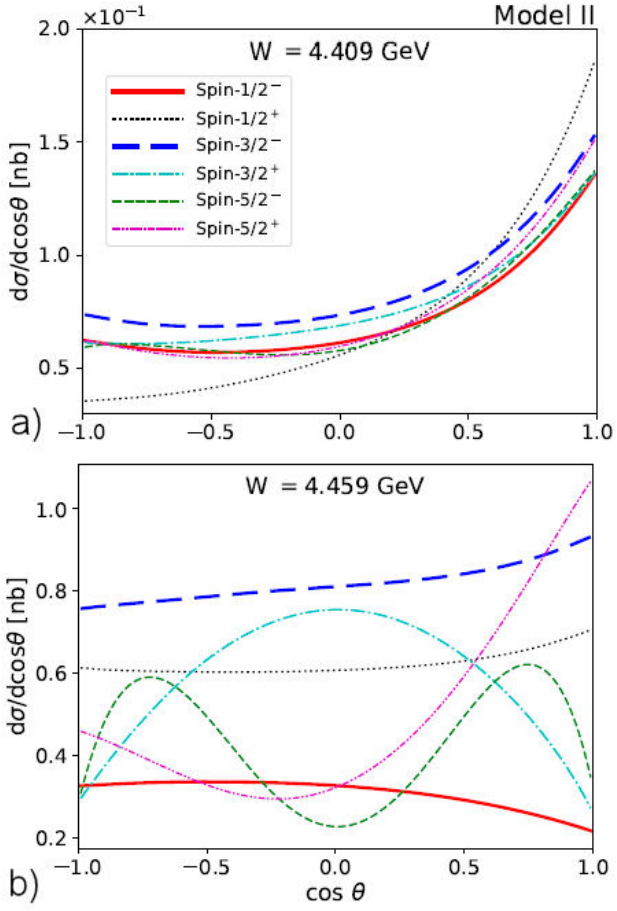

FIGURE 5. The calculated differential cross section ($d\sigma/d\Omega$) as a function of the scattering angle θ for a given total energy W from Model II by taking into account six different assignments of spin-parity quantum number of $P^0_{cs}(4459)$.

is sensitive to the spin and parity of the resonance. Nevertheless, this difference is not enough to distinguish the spin-parity quantum number of P_{cs} experimentally.

We also investigate the difference between Model I and II. Model I produces the total cross section which increases very slowly as the energy increases where it falls off fast, as the energy increases further due to the inclusion of form factor. On the other hand, Model II enhances the total cross section near the threshold and after the resonance region. As the energy increases, the results decrease, as expected. This shows that the Regge approach gives a better asymptotic behavior at high energy while the effective Lagrangian approach requires phenomenological form factors to achieve the similar results. If one takes a look closely, the result for P_{cs} with spin-$5/2^-$ yields different behavior, compared to the rest that appear not only in Model I but also in Model II. This peculiarity appears since the hadronic form factor used in the present work is not enough to suppress the high power momentum in the amplitude for spin-5/2 resonances. Actually, this unwanted behavior for the spin-$5/2^-$ case still exists at higher energy regions. However, we will not resolve this problem, since it is not our main concern in the present work.

In Figs. 4 and 5, we depict the differential cross section $d\sigma/d\Omega$ as a function of the scattering angle $\cos\theta$ with the total energy W from Model I and Model II fixed. At the resonance regions, one can clearly distinguish the shape of the graph from the results on different spin-parity quantum numbers of P_{cs} except those for the spin-$1/2^+$ and -$3/2^-$ cases. Both of them give almost similar shapes in the forward direction while their behavior differs slightly in the backward direction. In the vicinity of about 50 MeV above the resonance region, all the results give rather similar shapes. It is not surprising since the width of $P_{cs}(4459)$ is only about 17 MeV. Therefore, the experimental data on the differential cross section, especially near the resonance mass region, is really crucial in determining the spin-parity assignment of the hidden-charm strange pentaquark $P^0_{cs}(4459)$.

4. Conclusions

We investigated the production of hidden-charmed pentaquark with strangeness $P^0_{cs}(4459)$ by utilizing two different theoretical schemes, *i.e.*, the effective Lagrangian and hybridized Regge approach. By considering six different spin-parity quantum numbers of P_{cs}, we examined its effect on the total cross section and differential cross section. While it is hard to distinguish each spin-parity in the total cross section, we found the distinct difference in the differential cross section specifically around the resonance mass region. However, it will be hard to distinguish the results for spin-$1/2^+$ and -$3/2^-$, since their shapes are almost similar each other. Nevertheless, the present work may provide a helpful guidance for future experiments on finding the hidden-charmed pentaquark with strangeness P_{cs} and determining its quantum number.

5. Acknowledgments

The present work was supported by Basic Science Research Program through the National Research Foundation of Korea funded by the Korean government (Ministry of Education, Science and Technology, MEST), Grant-No. 2021R1A2C2093368 and 2018R1A5A1025563.

1. R. Aaij *et al.* [LHCb], Observation of $J/\psi p$ Resonances Consistent with Pentaquark States in $\Lambda_b^0 \to J/\psi K^- p$ Decays, *Phys. Rev. Lett.* **115** (2015) 072001.

2. R. Aaij *et al.* [LHCb], Observation of a narrow pentaquark state, $P_c(4312)^+$, and of two-peak structure of the $P_c(4450)^+$, *Phys. Rev. Lett.* **122** (2019) 222001.

3. R. Aaij *et al.* [LHCb], Evidence of a $J/\psi\Lambda$ structure and observation of excited Ξ^- states in the $\Xi_b^- \to J/\psi\Lambda K^-$ decay, *Sci. Bull.* **66** (2021) 1278-1287.
4. J. J. Wu, R. Molina, E. Oset and B. S. Zou, Prediction of narrow N^* and Λ^* resonances with hidden charm above 4 GeV, *Phys. Rev. Lett.* **105** (2010) 232001.
5. H. X. Chen, L. S. Geng, W. H. Liang, E. Oset, E. Wang and J. J. Xie, Looking for a hidden-charm pentaquark state with strangeness S=-1 from b^- decay into J/$\psi K^-\Lambda$, *Phys. Rev. C* **93** (2016) 065203.
6. E. Santopinto and A. Giachino, Compact pentaquark structures, *Phys. Rev. D* **96** (2017) 014014.
7. R. Chen, J. He and X. Liu, Possible strange hidden-charm pentaquarks from $\Sigma_c^{(*)}\bar{D}_s^*$ and $\Xi_c^{(',*)}\bar{D}^*$ interactions, *Chin. Phys. C* **41** (2017) 103105.
8. C. W. Shen, J. J. Wu and B. S. Zou, Decay behaviors of possible $\Lambda_{c\bar{c}}$ states in hadronic molecule pictures, *Phys. Rev. D* **100** (2019) 056006.
9. C. W. Xiao, J. Nieves and E. Oset, Prediction of hidden charm strange molecular baryon states with heavy quark spin symmetry, *Phys. Lett. B* **799** 135051 (2019).
10. B. Wang, L. Meng and S. L. Zhu, Spectrum of the strange hidden charm molecular pentaquarks in chiral effective field theory, *Phys. Rev. D* **101** (2020) 034018.
11. N. Brambilla, S. Eidelman, C. Hanhart, A. Nefediev, C. P. Shen, C. E. Thomas, A. Vairo and C. Z. Yuan, The XYZ states: experimental and theoretical status and perspectives, *Phys. Rept.* **873** (2020) 1-154.
12. A. Ali *et al.* [GlueX], First Measurement of Near-Threshold J/ψ Exclusive Photoproduction off the Proton, *Phys. Rev. Lett.* **123** (2019) 072001.
13. Q. F. Lü, X. Y. Wang, J. J. Xie, X. R. Chen and Y. B. Dong, Neutral hidden charm pentaquark states $P_c^0(4380)$ and $P_c^0(4450)$ in $\pi^- p \to J/\psi n$ reaction, *Phys. Rev. D* **93** (2016) 034009.
14. S. H. Kim, H.-Ch. Kim and A. Hosaka, Heavy pentaquark states $P_c(4380)$ and $P_c(4450)$ in the J/ψ production induced by pion beams off the nucleon, *Phys. Lett. B* **763**, (2016) 358-364.
15. M. Guidal, J. M. Laget and M. Vanderhaeghen, Pion and kaon photoproduction at high-energies: Forward and intermediate angles, *Nucl. Phys. A* **627**, (1997) 645-678.
16. S. H. Kim, A. Hosaka, H.-Ch. Kim, H. Noumi and K. Shirotori, Pion induced Reactions for Charmed Baryons, *PTEP* **2014** (2014) 103D01.
17. S. H. Kim, A. Hosaka, H.-Ch. Kim and H. Noumi, Production of strange and charmed baryons in pion induced reactions, *Phys. Rev. D* **92** (2015) 094021.
18. S. Clymton, H. J. Kim and H.-Ch. Kim, Production of hidden-charm strange pentaquarks Pcs from the *Phys. Rev. D* **104** (2021) 014023.
19. R. Chen, Strong decays of the newly $P_{cs}(4459)$ as a strange hidden-charm $\Xi_c\bar{D}^*$ molecule, *Eur. Phys. J. C* **81** (2021) 122.
20. C. W. Xiao, J. J. Wu and B. S. Zou, Molecular nature of $P_{cs}(4459)$ and its heavy quark spin partners, *Phys. Rev. D* **103** (2021) 054016.
21. P. A. Zyla *et al.* [Particle Data Group], Review of Particle Physics, *PTEP* **2020** (2020) 083C01.
22. T. A. Rijken, M. M. Nagels and Y. Yamamoto, Baryon-baryon interactions: Nijmegen extended-soft-core models, *Prog. Theor. Phys. Suppl.* **185**, (2010) 14-71.
23. T. Barnes and X. Li, Associated Charmonium Production in Low Energy p anti-p Annihilation, *Phys. Rev. D* **75**, (2007) 054018.
24. M. M. Brisudova, L. Burakovsky and J. T. Goldman, Effective functional form of Regge trajectories, *Phys. Rev. D* **61**, (2000) 054013.